ACS APPLIED MATERIALS & INTERFACES

Research Article

www.acsami.org

Construction of Polyfunctional Coatings Assisted by Gallic Acid to Facilitate Co-Immobilization of Diverse Biomolecules

Zhilu Yang,*[,†,‡,§] Ying Yang,[†,‡,§] Wei Yan,[†,‡] Qiufen Tu,*[,†,⊥] Jin Wang,*[,†,‡] and Nan Huang[†,‡]

[†]Key Laboratory of Advanced Technology for Materials of Education Ministry, [‡]The Institute of Biomaterials and Surface Engineering, School of Materials Science and Engineering, and [⊥]Laboratory of Biosensing and MicroMechatronicsSouthwest Jiaotong University, Chengdu, 610031, China

Supporting Information

ABSTRACT: Designing a multifunctional surface based on the coimmobilization of two or more diverse biomolecules with synergic action is very important in certain cases. In this work, a facile method by two-step aimed to construct a polyfunctional coating containing −COOH, $-NH_2$, and phenol/quinine groups was reported. The first-step was to introduce amine groups onto target modified-surface by coating with plasma polymerized allylamine (PPAam), followed by the second-step conjugation of gallic acid (3,4,5-trihydroxybenzoic acid) onto the PPAam surface. The density of −COOH, $-NH_2$, and phenol/quinone groups could be regulated easily by adjusting the reaction time of GA conjugation, making it possible to coimmobilize two or three diverse molecules. This has been shown by the successful coimmobilization of anti-CD34 antibody and vascular endothelial growth factor (VEGF). The surface coimmobilized with the anti-CD34 antibody and VEGF presented significant enhancement in the capture of endothelial progenitor cells (EPCs) and the growth of human umbilical vein endothelial cells (HUVECs). These data suggest the huge potential of such polyfunctional coating for tailoring the desired interfacial properties of materials through selectively conjugating two or more diverse bioactive molecules with synergic action.

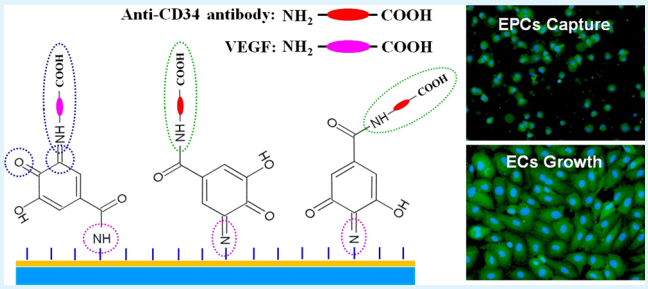

KEYWORDS: *multiple functional groups, biomolecules, coimmobilization, interfacial properties, multifunctional coating*

1. INTRODUCTION

Immobilization of biomolecules is a very important means to tailor the properties of the surface and has been widely utilized in molecular biology, analytical chemistry, bioprocess engineering, medical diagnostics, regenerated medicine, tissue engineering, and biomedical implants.[1−6] Especially, in certain cases, coimmobilization of diverse biomolecules with synergistic action is requested, e.g., a multifunctional surface on vascular stents or grafts coated with anti-CD34 antibody and VEGF to promote the rapid re-endothelialization and reduce the restenosis.[7−10]

Numerous methods existed for binding biomolecules onto the surface of biomaterials, such as physical adsorption,[11] self-assembly (including monolayer self-assembly and layer-by-layer (LBL) self-assembly),[12,13] anchoring,[14] and direct covalent immobilization.[15−17] Noncovalent and covalent strategies are two generally exploited methods to immobilize biomolecules. The former includes typical physical adsorption and electrostatic self-assembly, which require only a hydrophobic or electrostatic effect between the biomolecules and the materials surface.[13] These methods made it available to coimmobilize two or more diverse biomolecules onto a substrate surface. However, the major disadvantage of noncovalent method is the uncontrollable initial burst release of the target biomolecules from the substrate surface. Fortunately, the stability and persistence of the bound biomolecules could be considerably improved by covalent strategy. Compared with the noncovalent method, covalent immobilization can prolong the biomolecule availability, decrease the requirement of large amount of biomolecules, and prevent the burst release of a plenty of biomolecules, when applied out of a therapeutic concentration and cause damage to cells or tissues. Nevertheless, there must be a reactive group presented on the substrate surface, which rarely works for most alloys, inorganic materials, and many polymers. Recently, depositing organic thin films with reactive groups onto the surface of bulk material for binding biomolecules had attracted much attention.[18−20] Usually, only one type of reactive functional group presents on these organic thin films; the coimmobilization of two or more diverse biomolecules is challenging. Although some reports showed that two diverse biomolecules could be coimmobilized on such organic thin-film-coated substrate, the coimmobilization of diverse biomolecules were usually performed by immersing the target substrate into a solution mixed with biomolecules, and the amounts of biomolecules bound to the substrate could not be controlled.[21,22]

Received: May 27, 2013
Accepted: October 10, 2013
Published: October 10, 2013

Herein, we developed a novel and facile two-step approach for construction of polyfunctional coatings containing −COOH, $-NH_2$, and phenolic hydroxyl/quinone groups that can be used to selectively immobilize two or three different type of biomolecules. This processes first involved the introduction of amine groups by deposition of the PPAam coating on the modified-surface (Scheme 1A), followed by the second-step conjugation of GA (Scheme 1B) onto the PPAam film for constructing a polyfunctional surface (Scheme 1C).

Scheme 1. (A) Modification of 316L SS by the Deposition of the PPAam Film, (B) Oxidation of GA in Tris Buffer Solution; (C) Conjugation of GA on PPAam Coating

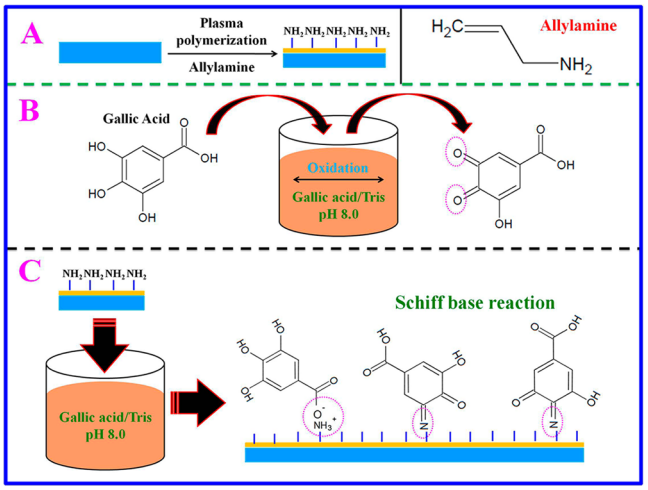

The particular plasma polymerization technique allows the formation of a thin pinhole-free and high homogeneous PPAam film with good surface coverage and strong adhesion strength on almost all materials, which also provides abundant reactive amine groups. GA (3,4,5-triphydroxyl-benzoic acid) with one carboxyl and three phenolic hydroxyl groups in the molecular is a biologically important and chemically unique phenolic acid. GA was particularly sufficient existed in beverages such as red wines[23] and green tea[24] and had strong antioxidant effects associated with the prevention of arteriosclerosis,[25] antibacterial,[26] antiviral,[27] and anti-inflammatory activity.[28] Of special interest is that Inoue and Qiu et al.[29,30] found that GA has the character of selective induction of cell death, showing the apoptotic effects on smooth muscle cells (SMCs) but no cytotoxicity against endothelial cells (ECs). GA was thereby chosen in this work to tailor the surface functionalities of the PPAam film for introducing additional reactive groups of carboxyl and phenolic hydroxyl/quinone groups. The process involved the chemical reaction between carboxyl and phenolic hydroxyl/quinone groups of the GA and the amine groups ($-NH_x$, x = 1, 2) of the PPAam (Scheme 1C). Of special importance is that the density of carboxyl (−COOH) and amine groups ($-NH_x$) can be easily controlled via the reaction time of GA conjugation.

2. EXPERIMENTAL SECTION

Preparation of PPAam Coating. 316L SS (Φ = 10 mm), the most widely used stent material was used to deposit the functional PPAam coating by using an inductively coupled plasma excited with an external copper band electrodes at a 13.56 MHz pulsed radio frequency (RF).[32] In this work, allylamine (purity ≥99.0%, Sigma) was chosen as precursor to prepare a functional film with abundant amine groups. Pulsed mode was used to tailor a high density of functional groups on PPAam coating. Before the plasma polymerization, 15 min of argon plasma sputtering was used to clean the vacuum chamber and the sample surface. The deposition parameters were set as 6.0 Pa system pressure composed of 2.5 Pa of Ar and 3.5 Pa of allylamine vapor, 80 V negative bias voltage, 30 W RF power, and 40% (t_{on} = 20 ms, t_{off} =30 ms) pulse duty cycle. Ultimately, the PPAam film with thickness of 100 nm was deposited on substrate via the control of the deposition time.[31]

GA Conjugation. In brief, the PPAam-coated 316L SS was immersed into 1 mg of GA (Purity ≥97.0%, Sigma) per 1 mL of Tris (2 mg/mL, Purity ≥99.0%, Sigma, pH 8.5) buffer for 12 h, and then rinsed with PBS (3 × 15 min) and distilled water (3 × 15 min) and ready for surface analysis.

Determination of Functional Groups. The samples of 316L stainless steel (SS) coated with PPAam were dipped in 1 mg/mL of GA in 10 mM Tris buffer (pH 8.5) for different periods of time and then washed with PBS and distilled water to obtain the GA-PPAam polyfunctional coatings. An Acid Orange II colorimetric staining method was used to determine the amine groups. First, samples of PPAam control and GA-PPAam (n = 4) were incubated in a 500 nM Acid Orange II (AO) aqueous solution at pH 3. After incubation for 12 h at 37 °C, the samples were washed (3 × 15 min) with hydrochloric acid solution (pH 3), then incubated in NaOH solution (pH 12) at 37 °C for 15 min to dissolve the combined AO adsorbed on the sample surface. The AO concentration in the NaOH solution was colorimetrically measured by a microplate reader (μQuant, Biotek instruments Inc.) at 485 nm. Toluidine blue-O (TBO) method was used to determine carboxyl groups. Initially, 40 μM TBO solution was prepared by dissolving TBO in NaOH solution (pH 10). Then the samples of PPAam control and GA-PPAam (n = 4) were incubated in the TBO solution for 12 h at 25 °C. Subsequently, the samples were washed with NaOH solution (3 × 15 min) to remove the physical adsorbed TBO, and 50 wt % acetic acid solution were used to dissolve the combined TBO on the samples surface. Ultimately, the concentration of the TBO in acid solution was examined by a microplate reader at 631 nm.

X-ray Photoelectron Spectroscopy (XPS) Measurement. The instrument of XSAM800 XPS (Kratos Ltd., UK) was used to analyze the surface chemical compositions of sample. XPS measurement was carried out using a monochromatic Al Kα (1486.6 eV) X-ray source, and operated at 12 kV × 15 mA at a pressure of 2×10^{-7} Pa. Here, charge correction was performed by a reference of the C 1s peak (binding energy 284.8 eV). The detailed information of XPS measurement were as shown elsewhere.[32]

Co-immobilization of Anti-CD34 Antibody and VEGF. After 12h of conjugation of GA in Tris buffer, the obtained GA-PPAam coated 316L SS was activated in a water-soluble carbodiimide (WSC) solution (pH 5.4) consisting of 9.76 mg/mL 2-(N-morpholino)-ethanesulfonic acid hydrate (MES, Purity ≥97.0%, Sigma-Aldrich), 1 mg/mL N-(3-dimethylaminopropyl)-N′-ethylcarbodiimide (EDC, Purity ≥98.0%, BIO Basic Inc.), and 0.24 mg/mL N-hydroxysuccinimide (NHS, Purity ≥97.0%, Sigma-Aldrich) for about 60 min, and then transferred into a MES solution containing 5 μg/mL anti-CD34 antibody (Wuhan Boster Biological Technology, Wuhan, China) for 70 min. After washing with PBS, the obtained specimens were transferred into PBS (pH7.4) buffer containing 500 ng/mL of VEGF (Purity ≥98.0%, PEPROTECH Inc. USA). Ninety minutes later, the specimens were fully rinsed with PBS and distilled water.

Real Time Monitoring of Anti-CD34 Antibody and VEGF Co-immobilization. Briefly, AT-cut 5 MHz Au coated quartz crystal (diameter: 10 mm) was first deposited by a 100 nm of PPAam film. After 12 h conjugation of GA in Tris buffer, the obtained GA-PPAam coated quartz crystal was settled in the quartz crystal microbalance with dissipation (QCM-D) chamber and a PBS (pH 7.4) solution was injected continuously at a rate of 50 μL/min until the QCM traces maintained steady. A WSC solution (pH =5.4) was subsequently injected in the same speed for activating −COOH of GA-PPAam, and then 5 μg of Anti-CD34 antibody per 1 mL of MES solution was injected in the same speed. After PBS rinsing, 500 ng of VEGF per 1

mL PBS buffer (pH 7.4) was injected in the same speed, finally washed with PBS. The calculation method of the mass of molecules bound to the surface was shown elsewhere.[32]

Fourier Transform Infrared (FTIR) Measurements. FTIR measurements were carried out with a Nicolet model 5700 instrument. Here, grazing angle attenuated total reflection accessory (GATR) was used. For propose of well compare the chemical structure difference of the specimens, the PPAam before and after conjugation of biological molecules of GA, anti-CD34 antibody, and VEGF were in sequence measured by FTIR instrument.

Isolation and Culture of EPC from Bone Marrow. A one-month-old Sprague−Dawley rat was euthanized by cervical dislocation, and the femurs were isolated. Bone marrow was flushed from the femurs using α-MEM culture medium with 10% fetal bovine serum (FBS) and fully dispersed. Histopaque 1077 (5 mL) was added to each 15 mL centrifuge tube, and isovolumetric bone marrow mixture was carefully layered upon. The centrifuge tubes were centrifuged at 2000 rpm for 20 min. Mononuclear cells were collected from the plasma-Histopaque 1077 interface layer, washed 2 times with α-MEM culture medium, and resuspended using α-MEM culture medium with 20% FBS, 10 ng/mL VEGF, 20 μg/mL endothelial cell growth supplement (ECGS) and cultured on a fibronectin-coated dish at 37 °C under 5% CO_2. Floating cells were removed after 48 h and the culture medium was changed each two days. When the confluence reached 80%, subculture was performed. The cells used in experiments were during third and fifth passage.

Dynamic Capture of EPCs. The dynamic capture of EPCs was carried out in a flow chamber as shown in Scheme S1 in the Supporting Information. The flow chamber system provides a laminar flow through a 1.5 mm gap between two parallel plates. The flow is provided by a roller pump, connected with polyvinyl chloride (PVC) tubes. Briefly, the samples (the size of sample: Φ10 mm) were prepared, and then 50 mL suspension of EPCs (5×10^4 cells/cm^2) was filled and pumped at 37 °C for 2 h at a flow rate of 65 mL/min (approximating coronary flow[33]). Subsequently, the samples were rinsed by PBS and fixed in 4% paraformaldehyde. Double fluorescence stained for both CD31 and DAPI to visualize the adherent or captured EPCs. The samples were subsequently inspected by using Olympus IX51 fluorescence microscope (Japan).

Immunostaining for Actin of HUVECs. The detailed process of HUVEC culture shows elsewhere.[32] HUVECs were cultured with the specimens at a density of 5×10^4 cells/cm^2, with incubation time set as 1 and 3 days. Then the specimens were washed with PBS and fixed in 4% paraformaldehyde. For actin immunostaining, the detailed process could be referred in our previous work.[32] The morphology of cells were analyzed and photographed by Olympus IX51 fluorescence microscope.

HUVEC Proliferation. The proliferation of the HUVECs grown on the samples was measured by Cell Counting Kit-8 (CCK-8) at the predetermined time 1 and 3 days respectively. Replace the medium with 350 μL fresh M199 medium (supplemented with 5% FBS and 20 μg/mL ECGS but without phenol red) containing 10% CCK-8 reagent for each specimens and incubate for 3 h 37 °C in standard culture conditions. Subsequently, 200 μL of these solutions were collected in a 96-well plate and the absorbance was measured in a microplate reader at 450 nm. The parallel samples were not less than four and the proliferation assays were performed twice.

3. RESULTS AND DISCUSSION

In this study, the determination of the densities of −COOH and $-NH_x$ was carried out using colorimetric staining with Acid Orange II and toluidine blue respectively. As shown in Figure 1, the density of −COOH gradually increased with the reaction time while the corresponding decrease in the density of $-NH_x$ was observed, suggesting the successful immobilization of GA to PPAam film. The presence of −COOH confirmed the Schiff base reaction between quinone of GA and amine groups of PPAam. It was noted that when the reaction time exceeded 4 h,

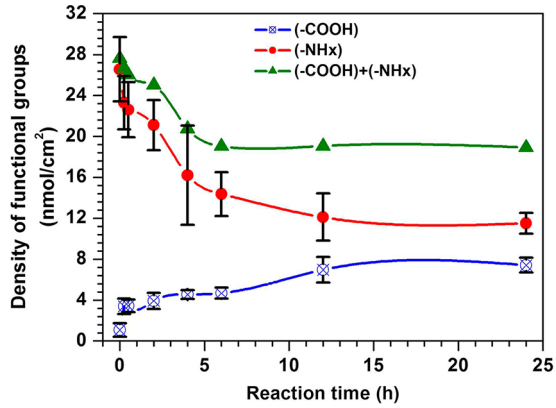

Figure 1. Density of carboxyl (−COOH) and amine ($-NH_x$, x = 1, 2) groups of PPAam coating before and after GA conjugation (the reaction time ranged from 15 min to 24 h).

the density of $-NH_x$ sharply reduced without corresponding significant increase in the density of −COOH. In addition, the total density of −COOH and $-NH_x$ showed a decreased tendency during the whole process of reaction, with a remarkable decay of the total amount of functional groups after reaction time of 4 h. The data suggested the presence of another chemical reaction for GA conjugation, i.e., the salt formation reaction between carboxyl of GA and primary amine groups of PPAam. After 12 h, the value of the density of −COOH, $-NH_x$ remained unchanged, suggesting the complete consumption of reactive amine groups. It is worth mentioning that although the total density of −COOH and $-NH_x$ reduced with the increase in reaction time, the introduction of phenolic hydroxyl/quinone groups derived from GA (see Figure S1 in the Supporting Information) could well-compensate this decay.

To further demonstrate the successful conjugation of GA to PPAam, we performed XPS analysis. The chemical compositions revealed a significant decrease in the content of nitrogen and increase in oxygen content, indicating the successful conjugation of GA to PPAam (Table 1). Here the further

Table 1. Chemical Compositions of the PPAam and GA-PPAam (the conjugation time of GA was 12 h) (n = 3)

sample	C (at %)	N (at %)	O (at %)
GA (nominal value)	58.3		41.7
PPAam	76.7 ± 0.3	16.7 ± 0.2	6.6 ± 0.4
GA-PPAam	75.6 ± 0.1	13.1 ± 0.4	11.3 ± 0.1

analysis of high-resolution C1s, N1s and O1s XPS spectra was performed to gain an insight into the reaction mechanisms of GA bound to the PPAam. The detections of the terminal aromatic −COOH of GA-PPAam at 288.5 (Figure 2A) and 534.2 eV (Figure 2C), and of reinforced peak at 399.5 eV (Figure 2B) (ascribe to the formation of aromatic C═N) revealed the Schiff base reaction of quinone groups derived from GA with amine groups of PPAam. In addition to Schiff base reaction, the other type of reaction, salt forming reaction between −COOH and $-NH_2$ was detected, as directly evidenced by the detection of the characteristic peak of the $-NH_3^+$ at 401.7 eV (Figure 2B).[34] Other important evidence supporting GA bound to PPAam such as FTIR, water contact angles (WCAs), and zeta potential are provided in Figure 3 and Figure S2 and Table S1 in the Supporting Information,

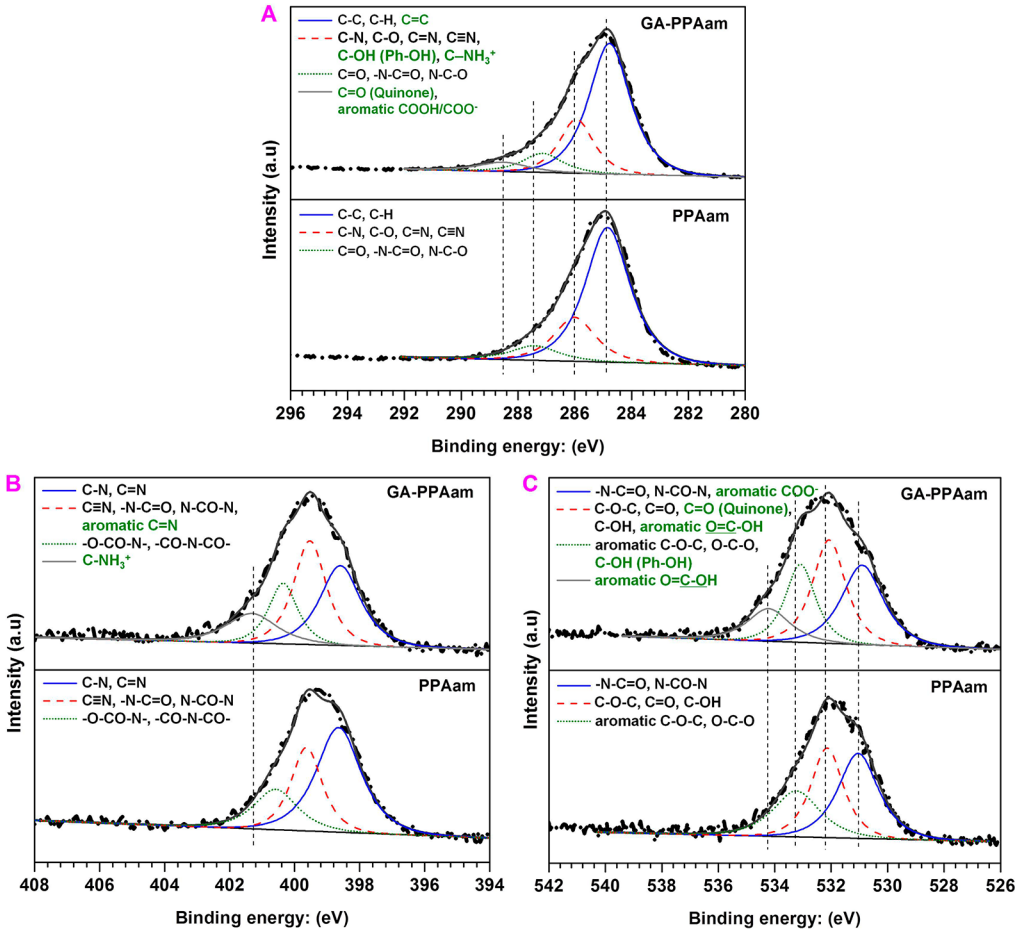

Figure 2. High-resolution XPS spectra of the (A) C1s, (B) N1s, and (C) O1s of the PPAam and GA-PPAam coatings.

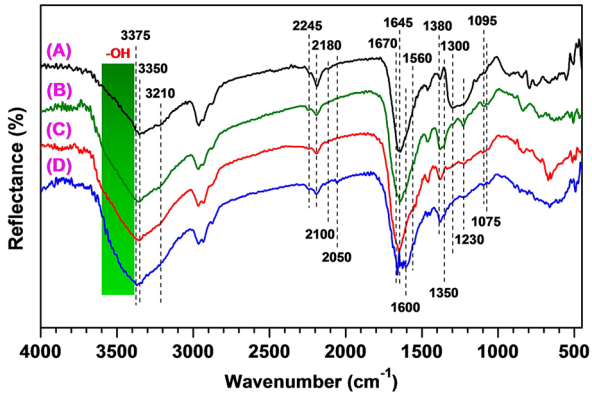

Figure 3. GATR-FTIR spectroscopy of (A) PPAam, (B) GA-PPAam, (C) anti-CD34 antibody immobilized, and (D) anti-CD34 antibody/VEGF coimmobilized surface (see Table S3 in the Supporting Information for complete peak assignments).

respectively. As shown in Figure 3 and Figure S4 in the Supporting Information, after GA immobilization, significant difference emerged in the chemical structure. The presence of aromatic O−H deformation and aromatic C−O stretching vibrations (at 1350 and 1260−1180 cm^{-2}), aromatic C═H deformation vibration (at 1095 cm^{-2}), and aromatic C═O stretching vibration in carboxylic acids (at 1690 cm^{-2}) and reinforce of the absorption band around 3600−3100 cm^{-2} (ascribe to the presence of the −COOH of GA) strongly confirmed the introduction of GA to the PPAam surface.

Here, anti-CD34 antibody and VEGF were chosen as target biomolecules to coimmobilize on GA-PPAam to test the availability of functional groups on its surface. To accelerate the spontaneous endothelialization of vascular implants is considered to be one of the most promising approaches to address issues associated with the surface-induced thrombosis and restenosis. Capturing circulating EPCs from blood for inducing in situ endothelialization has thereby been proposed and highlighted in recent studies.[7] As a number of special marker of EPC (a $CD34^+$ cell), anti-CD34 antibody has been developed to modify the vascular stents for in situ inducing re-endothelialization.[7,9,10] Though the anti-CD34 antibody coated stents have been reported to show a significantly enhanced influence on the adhesion and proliferation of EPCs in vitro and on the capture and attachment of EPCs in vivo, clinical long-term studies revealed that the antirestenotic effects of coated stents were not as remarkable as expected[31] possibly because of the difficulties to accurately control the differentiation of EPCs.[35] VEGF, a crucial molecule, which play an important role in regulating cell signaling, proliferation, migration, and differentiation,[36] and can significantly promote the adhesion and proliferation of ECs.[37−39] Therefore, the coimmobilization of anti-CD34 antibody and VEGF with synergic action may be a promising strategy to promote the rapid re-endothelialization and reduce restenosis of vascular stents or grafts.

Here, the GA-PPAam equipped with reactive groups of −COOH and phenolic hydroxyl/quinone groups obtained after

12 h of GA conjugation was used to accomplish the coimmobilization of anti-CD34 antibody and VEGF. Panels A and B in Figure 4 show that in the case of conjugation of anti-

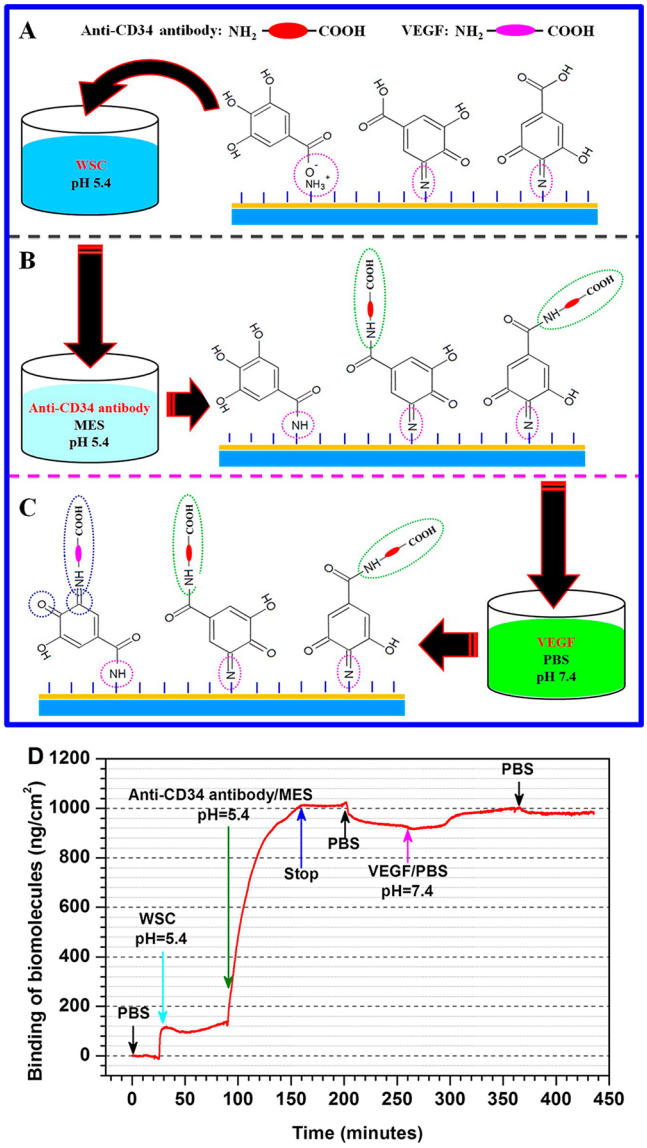

Figure 4. (A) Carboxyl groups of GA-PPAam were activated by EDC/NHS in water-soluble carbodiimide (WSC) solution. (B) Conjugation of anti-CD34 antibody on activated GA-PPAam coating. (C) Conjugation of VEGF on GA-PPAam coating. (D) QCM-D analysis for the coimmobilization of anti-CD34 antibody and VEGF to GA-PPAam surface.

CD34 antibody, the −COOH of GA-PPAam was activated by EDC/NHS in advance (in this step, the salt bond formed by −COOH of GA and $-NH_2$ of PPAam in Tris buffer was broken, and amide bond was formed due to the activation of carboxyl group by EDC/NHS (as shown in Figure S3 in the Supporting Information), which increased the stability of GA immobilized on PPAam), and then the anti-CD34 antibody in MES buffer was added without EDC/NHS to avoid the cross-linking of anti-CD34 antibody that damage its activity. The VEGF conjugation was based on a simple one-step Schiff base reaction between the quinone groups of GA-PPAam and amine groups of VEGF in PBS (pH 7.4, physiological pH value). Ultimately, 968 ± 36 ng/cm^2 of anti-CD34 antibody and 76 ± 9 ng/cm^2 of VEGF were successfully coimmobilized on GA-PPAam surface, as determined by QCM-D and confirmed by the tests of chemical composition (see Table S2 in the Supporting Information), WCAs (see Figure S2 in the Supporting Information), and chemical structure (Figure 3). Comparing the FTIR of GA-PPAam before and after conjugation of anti-CD34 antibody, an absorbing band of NH_3^+ around 1580−1500 cm^{-2} corresponding to the amino acid was observed (see Figure S4, right picture, in the Supporting Information), which confirmed the conjugation of anti-CD34 antibody. After further immobilization of VEGF the absorbing band of NH_3^+ around 1580−1500 cm^{-2}, amide I and amide II were further reinforced, indicating the successful conjugation of VEGF.

The bioactivity of anti-CD34 antibody and VEGF bound to the GA-PPAam surface were evaluated by the experiments of the specific capture of EPCs and the EC proliferation. As expected, the GA-PPAam conjugated with single anti-CD34 antibody showed a substantial enhancement in EPC capture as compared with the control 316L SS, PPAam and GA-PPAam (Figure 5A), and no significant promotion in EPC capture on

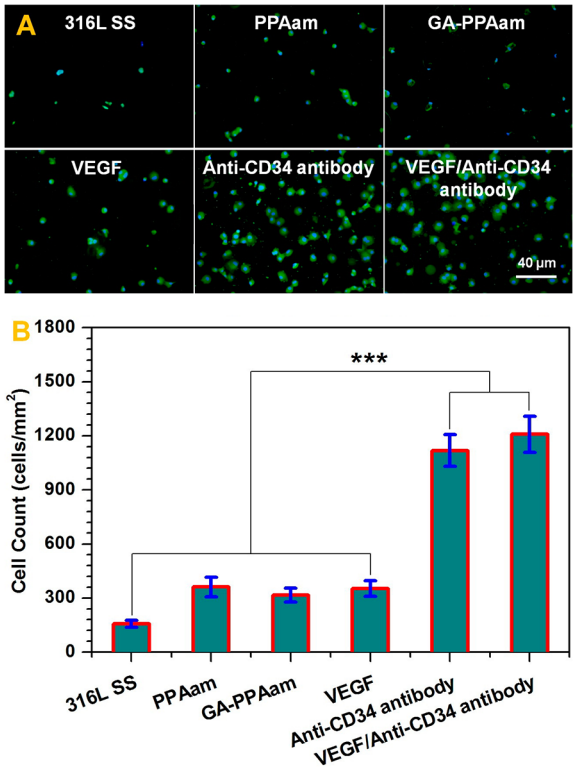

Figure 5. (A) DAPI and CD31 immunostaining of captured EPCs on the 316L SS, PPAam and GA-PPAam surfaces before and after single conjugation of Anti-CD34 antibody, VEGF and coimmobilization of Anti-CD34 antibody and VEGF after 2 h of flow chamber experiment under flow condition. (B) Amounts of captured EPCs calculated from at least 12 images. Data presented as mean ± SD and analyzed using a one-way ANOVA, ***$p < 0.001$.

its surface after further immobilization of VEGF, but little increase in the number of captured EPCs based on statistical results (Figure 5B). This indicates that the anti-CD34 antibody bound to the surface shows the good bioactivity.

The attachment and proliferation of HUVECs were carried out to evaluate the bioactivity of the VEGF conjugated to the

GA-PPAam. Figure 6A shows the typical fluorescence microscopic images of HUVECs after 1 day of culture. Clearly, the

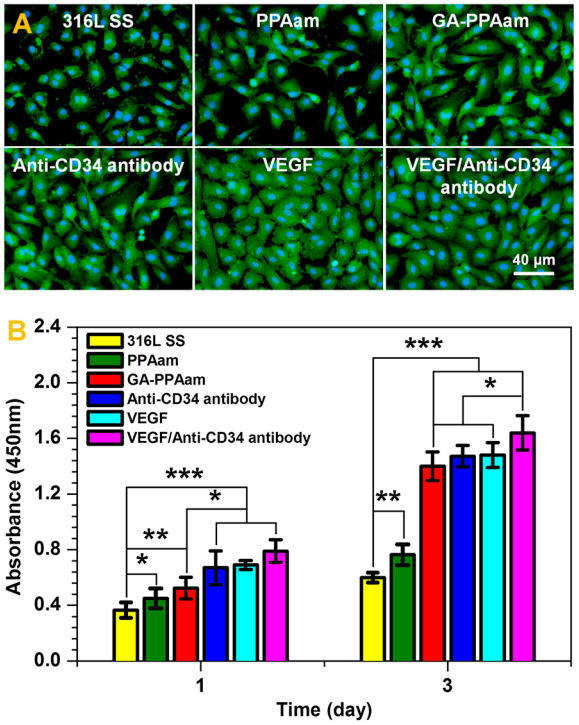

Figure 6. (A) Cytoskeletal actin (green) and nuclear (blue) stains of HUVECs on the 316L SS, PPAam, GA-PPAam before and after single conjugation of anti-CD34 antibody, VEGF, and coimmobilization of anti-CD34 antibody and VEGF after culture for 1 day. (B) Proliferation of HUVECs after 1 and 3 days' culture determined by Cell Counting Kit-8. Data presented as mean ± SD and analyzed using a two-way ANOVA, $*p < 0.05$, $**p < 0.01$, $***p < 0.001$.

GA-PPAam surfaces conjugated with single VEGF significantly promoted HUVEC growth as compared to the GA-PPAam. The surface also remarkably promoted the proliferation of HUVECs after 1 day of culture, however, no significant difference between them increased with culture time (Figure 6B). Note that the GA-PPAam immobilized with single anti-CD34 antibody also remarkably enhanced HUVEC adhesion and proliferation compared with the GA-PPAam. After further conjugation of VEGF, it presented a further increase in the proliferation of HUVEC as compared with the GA-PPAam surfaces conjugated with single anti-CD34 antibody or VEGF. These results suggest a good bioactivity of VEGF coimmobilized with anti-CD34 antibody on GA-PPAam surfaces.

4. CONCLUSIONS

In summary, we successfully fabricated a polyfunctional coating decorated with −COOH, $-NH_2$, and phenolic hydroxyl/quinone groups to accomplish the coimmobilization of two diverse biomolecules. This technology of the biomolecule coimmobilization is superior to that reported previously.[21,22] The coimmobilization of biomolecules reported in this work can be well carried out step-by-step using different reactive groups and reaction mechanism, and the amounts of biomolecules bound to the surface can also be regulated and controlled by adjusting the amounts of reactive groups. The polyfunctional coating of GA-PPAam shows the huge potential in tailoring the desired interfacial properties onto a wide range of materials through the selective coimmobilization of two or more diverse biomolecules with synergistic action.

■ ASSOCIATED CONTENT

Supporting Information

Scheme S1 for the schematic illustration of EPC capture using flow chamber; Figure S1 for the phenolic hydroxyl/quinone groups of the GA-PPAam; Table S1 for the zeta potential of the 316L SS, PPAam, and GA-PPAam coatings; Figure S2 and Table S2 for the WCAs and the chemical compositions of the PPAam, GA-PPAam, anti-CD34 antibody immobilized, and anti-CD34 antibody/VEGF coimmobilized surface; Figure S3 for the high-resolution N1s XPS spectra of GA-PPAam and GA-PPAam[1] (after further treatment with EDC/NHS) coatings; Figure S4 for FTIR of (A) PPAam, (B) GA-PPAam, (C) anti-CD34 antibody immobilized, and (D) anti-CD34 antibody/VEGF coimmobilized surface; Table S3 for the assignment of infrared spectra. This material is available free of charge via the Internet at http://pubs.acs.org.

■ AUTHOR INFORMATION

Corresponding Authors

*E-mail: zhiluyang1029@126.com. Tel: +86 28 87634148-803; Fax: +86 28 87600625.
*E-mail: tqfyezi7895@gmail.com.
*E-mail: jinxxwang@263.net.

Author Contributions

§Z.Y. and Y.Y. are co-first authors.

Notes

The authors declare no competing financial interest.

■ ACKNOWLEDGMENTS

This work was supported by the NSFC (Project 81271701 and 51173149), the Ministry of Science and Technology of China (Key Basic Research Project 2011CB606204), and NSFC Key Program 81330031.

■ REFERENCES

(1) Hodneland, C. D.; Lee, Y.-S.; Min, D.-H.; Mrksich, M. *Proc. Natl. Acad. Sci. U.S.A.* **2002**, *99*, 5048−5052.
(2) Robinson, D. E.; Marson, A.; Short, R. D.; Buttle, D. J.; Day, A. J.; Parry, K. L.; Wiles, M.; Highfield, P.; Mistry, A.; Whittle, J. D. *Adv. Mater.* **2008**, *20*, 1166−1169.
(3) Sanghvi, A. B.; Miller, K. P-H.; Belcher, A. M.; Schmidt, C. E. *Nat. Mater.* **2005**, *4*, 496−502.
(4) Lee, J. S.; Johnson, A. J. W.; Murphy, W. L. *Adv. Mater.* **2010**, *22*, 5494−5498.
(5) Alberti, K.; Davey, R. E.; Onishi, K.; George, S.; Salchert, K.; Seib, F. P.; Bornhäuser, M.; Pompe, T.; Nagy, A.; Werner, C.; Zandstra, P. W. *Nat. Methods* **2008**, *5*, 645−650.
(6) Yang, Z. L.; Wang, J.; Luo, R.; Maitz, M. F.; Jing, F.; Sun, H.; Huang, N. *Biomaterials* **2010**, *31*, 2072−2083.
(7) Avci-Adali, M.; Paul, A.; Ziemer, G.; Wendel, H. P. *Biomaterials* **2008**, *29*, 3936−3945.
(8) Meng, S.; Liu, Z.; Shen, L.; Guo, Z.; Chou, L. L.; Zhong, W.; Du, Q.; Ge, J. *Biomaterials* **2009**, *30*, 2276−2283.
(9) Lin, Q.; Ding, X.; Qiu, F.; Song, X.; Fu, G.; Ji, J. *Biomaterials* **2010**, *31*, 4017−4025.
(10) Li, Q. L.; Huang, N.; Chen, C.; Chen, J.; Xiong, K.; Chen, J.; You, T.; Jin, J.; Liang, X. *J. Biomed. Mater. Res. A.* **2010**, *4*, 1283−1293.
(11) Patil, S. D.; Papadmitrakopoulos, F.; Burgess, D. J. *J. Controlled Release* **2007**, *117*, 68−79.
(12) Liu, Q.; Ding, J.; Mante, F. K.; Wunder, S.; Baran, G. R. *Biomaterials* **2002**, *23*, 3103−3111.

(13) Decher, G. *Science* **1997**, *277*, 1232−1237.
(14) Ye, Q.; Zhou, F.; Liu, W. M. *Chem. Soc. Rev.* **2011**, *40*, 4244−4258.
(15) Zouani, O. F.; Chollet, C.; Guillotin, B.; Durrieu, M. *Biomaterials* **2010**, *31*, 8245−8253.
(16) Leslie-Barbick, J. E.; Shen, C.; Chen, C.; West, J. L. *Tissue Eng., Part A* **2011**, *17*, 221−229.
(17) Lin, C.; Anseth, K. S. *Pharm. Res.* **2009**, *26*, 631−643.
(18) Siow, K. S.; Britcher, L.; Kumar, S.; Griesser, H. J. *Plasma Process. Polym.* **2006**, *3*, 392−418.
(19) Lee, H.; Dellatore, S. M.; Miller, W. M.; Messersmith, P. B. *Science* **2007**, *318*, 426−430.
(20) Hilf, S.; Kilbinger, A. F. M. *Nat. Chem.* **2009**, *1*, 537−546.
(21) Lee, Y. B.; Shin, Y. M.; Lee, J.; Jun, I.; Kang, J. K.; Park, J. C. *Biomaterials* **2012**, *33*, 8343−8352.
(22) Nilsson, P. H.; Ekdahl, K. N.; Magnusson, P. U.; Qu, H. C.; Iwata, H.; Ricklin, D. *Biomaterials* **2013**, *4*, 985−994.
(23) Ho, C. T.; Chen, Q.; Shi, H.; Zhang, K. Q.; Rosen, R. T. *Prev. Med.* **1992**, *21*, 520−525.
(24) Abu-Amsha Caccetta, R.; Burke, V.; Mori, T. A.; Beilin, L. J.; Puddey, I. B.; Croft, K. D. *Free Radical Biol. Med.* **2001**, *30*, 636−642.
(25) Urizzi, P.; Monje, M. C.; Souchard, J. P.; Abella, A.; Chalas, J.; Lindenbaum, A.; Vergnes, L.; Labidalle, S.; Nepveu, F. *J. Chim. Phys.* **1999**, *96*, 110−115.
(26) Kang, M. S.; Oh, J. S.; Kang, I. C.; Hong, S. J.; Choi, C. H. *J. Microbiol.* **2008**, *46*, 744−750.
(27) Kratz, J. M.; Andrighetti-Frohner, C. R.; Leal, P. C.; Nunes, R. J.; Yunes, R. A.; Trybala, E. *Biol. Pharm. Bull.* **2008**, *31*, 903−907.
(28) Kim, S. H.; Jun, C. D.; Suk, K.; Choi, B. J.; Lim, H.; Park, S. *Toxicol. Sci.* **2006**, *91*, 123−131.
(29) Inoue, M.; Suzuki, R.; Sakaguchi, N.; Li, Z.; Takeda, T.; Ogihara, Y. *Biol. Pharm. Bull.* **2007**, *18*, 1526−1530.
(30) Qiu, X. B.; Takemura, G.; Koshiji, M.; Hayakawa, H. Y.; Kanoh, M.; Maruyama, R. *Heart Vessels* **2000**, *15*, 90−99.
(31) Aoki, J.; Serruys, P. W.; van Beusekom, H.; Ong, A. T. L.; McFadden, E. P.; Sianos, G. *J. Am. Coll. Cardiol.* **2005**, *45*, 1574−1579.
(32) Yang, Z. L.; Tu, Q. F.; Wang, J.; Lei, X. J.; He, T. T.; Sun, H.; Huang, N. *Macromol. Biosci.* **2011**, *11*, 797−805.
(33) Berne, R. M.; Levy. M. N. *Cardiovascular Physiology*, 6th ed.; Mosby-Year Book: St. Louis, MO, 1992, *30*, 81−93.
(34) Yang, Z. L.; Lei, X. J.; Wang, J.; Luo, R. F.; He, T. T.; Sun, H.; Huang, N. *Plasma Process. Polym.* **2010**, *8*, 208−214.
(35) Hill, J. M.; Zalos, G.; Halcox, J. P. J.; Schenke, W. H.; Waclawiw, M. A.; Quyyumi, A. A. *New Engl. J. Med.* **2003**, *348*, 593−600.
(36) Peichev, M.; Naiyer, A. J.; Pereira, D.; Zhu, Z.; Lane, W. J.; Williams, M.; Oz, M. C.; Hicklin, D. J.; Witte, L.; Moore, M. A. S.; Rafii, S. *Blood* **1999**, *95*, 952−958.
(37) Poh, C. K.; Shi, Z.; Lim, T. Y.; Neoh, K. G.; Wang, W. *Biomaterials* **2010**, *31*, 1578−1585.
(38) Rahman, N.; Purpura, K. A.; Wylie, R. G.; Zandstra, P. W.; Shoichet, M. S. *Biomaterials* **2010**, *31*, 8262−8270.
(39) Anderson, S. M.; Chen, T. T.; Iruela-Arispe, M. L.; Segura, T. *Biomaterials* **2009**, *30*, 4618−4628.